

Wedge-Shaped BGO Scintillation Crystal For Positron Emission Tomography: Concise Communication

Z. H. Cho, H. S. Lee, and K. S. Hong

Korea Advanced Institute of Science, Seoul, Korea

In order to increase the detection efficiency and also reduce the interdetector spillage, a new wedge-shaped BGO scintillation detector array is proposed. By shaping the front part of a detector as a wedge, the absorption path becomes longer, particularly for obliquely incident photons, thereby improving the uniformity in the sensitivity for the incident photons of different angles. To demonstrate the effectiveness of the proposed detector shape, a Monte Carlo simulation was performed and the results are presented.

J Nucl Med 25: 901-904, 1984

Current trends in instrumentation for positron emission tomography are towards higher resolution and sensitivity, ultimately aiming for dynamic function studies with multislice or volume imaging capability (1-5). High-resolution imaging, in particular, requires the use of narrow detecting crystals while still retaining high enough detection efficiency. Bismuth germanate (BGO) crystals have been used successfully for this purpose (6-7) and a spatial resolution of 6-8 mm has been obtained. Even with BGO, however, if the crystal width is reduced to several millimeters, degradation of detection efficiency and interdetector spillage becomes significant, particularly with obliquely incident photons (8-11). The effect on the reconstructed image appears as a degradation of resolution and contrast toward the periphery of the object. Further narrowing of the crystal width, therefore, has encountered constraints. Alleviation of such a problem can be achieved by modification of the detector shape from the conventional parallelepiped to one with a wedge-shaped front end (Figs. 2 and 3). The proposed shape makes the absorption length longer for obliquely incident photons, thus increasing the detection efficiency and suppressing interdetector spillage. To confirm the expected improvement, a Monte Carlo simulation has been performed and the results are presented.

Received Jan. 13, 1984; revision accepted Apr. 2, 1984.

For reprints contact: Z. H. Cho, PhD, Dept. of Electrical Science; Korea Advanced Institute of Science, Seoul, Korea.

DESCRIPTION OF DETECTOR AND MONTE CARLO SIMULATIONS

A circular-ring positron tomograph consisting of wedge-shaped detectors is sketched in Fig. 1. The maximum oblique angle of the incident photon, θ , beyond which no photons are possibly incident, is indicated and given by

$$\theta = \sin^{-1}(R_0/R_D)$$

where R_D and R_0 represent radii of the system and the object (or field of view), respectively. In Fig. 2, a con-

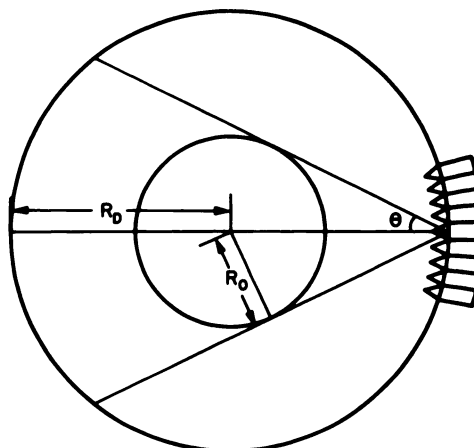


FIG. 1. Illustration of circular-ring positron emission tomograph with wedge-shaped BGO detectors. $\theta = \sin^{-1}(R_0/R_D)$ denotes maximum angle of incidence.

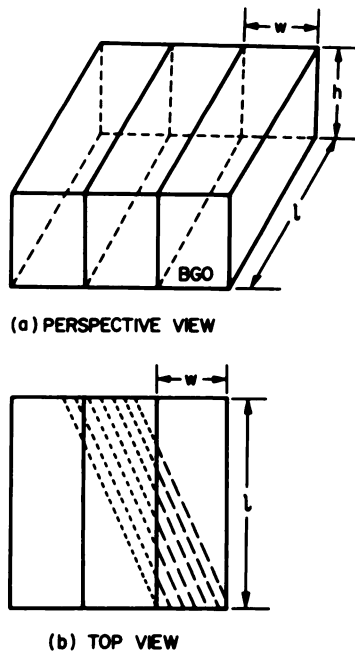


FIG. 2. Illustration of conventional detector arrangement. In (b) absorption length of crystal is indicated by broken lines and spillage by dotted lines. Note large range of absorption length for obliquely incident photons.

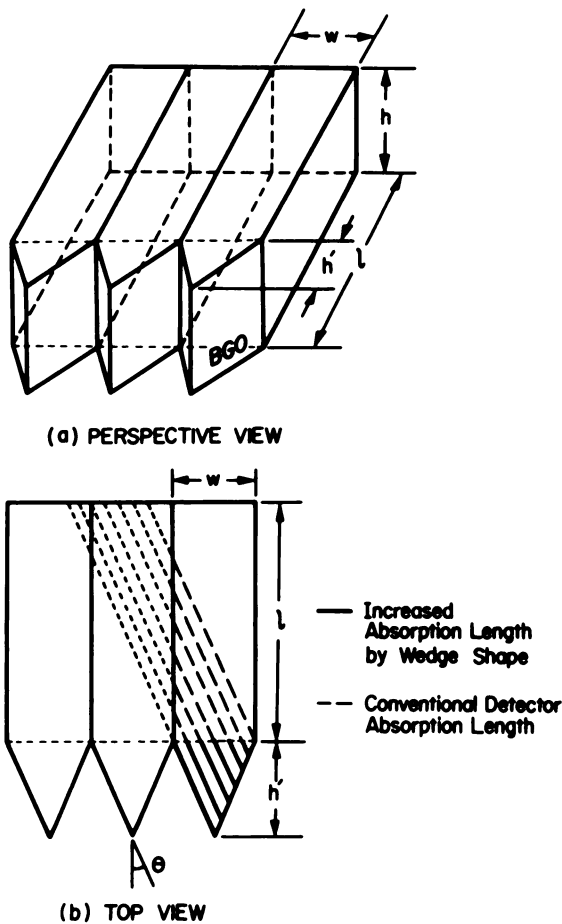


FIG. 3. Illustration of proposed wedge-shaped detector arrangement. Wedge angle θ is made equal to maximum angle of incident photons.

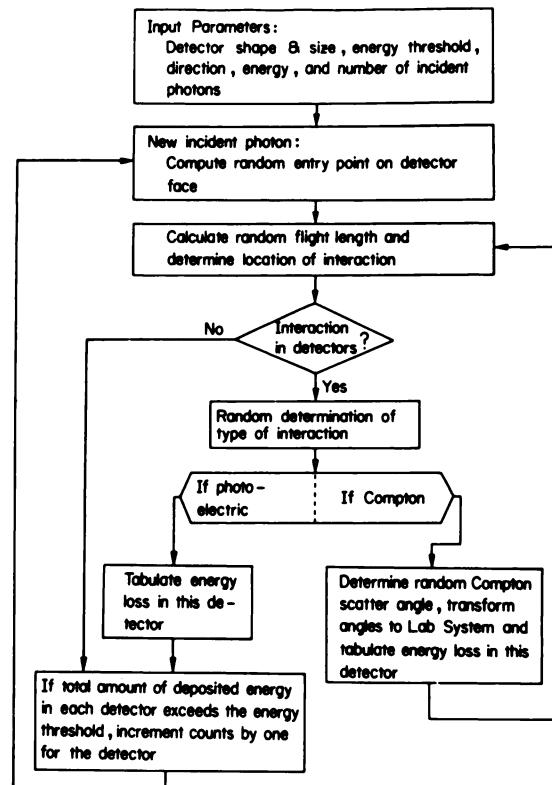


FIG. 4. Flow chart of Monte Carlo simulation program (computer program available upon request).

ventional detector arrangement is illustrated, with parameters where the large variation of absorption path length is clearly apparent (b). Note that a large fraction of photons obliquely incident towards the edge are spilled into the adjacent detector. By using the proposed wedge-shaped detector arrangement (Fig. 3), where wedge angle is taken to be equal to the maximum oblique incidence angle given by Eq. (1), absorption lengths can be roughly equalized and detection efficiency is thus increased compared with the conventional crystal shape.

To quantify the improvement in detector efficiency and interdetector spillage in the wedge-shaped crystal compared with the conventional shape, a Monte Carlo simulation has been performed. A flow chart of its computer program is shown in Fig. 4. The photoelectric interaction, Compton scatter, and Compton-plus-photoelectric absorption have been taken into account by tracing each incident photon until it escapes from the detector array or is completely absorbed. Annihilation photons of 511 keV are projected on the incident face of one detector, and the beam widths are kept the same for both crystal shapes. That is, photons are projected uniformly on the plane of the front face of the rectangular type as well as the wedge-shaped detector (Figs. 2 and 3).

In the present study, bismuth germanate is assumed as the detector material and detectors are closely packed,

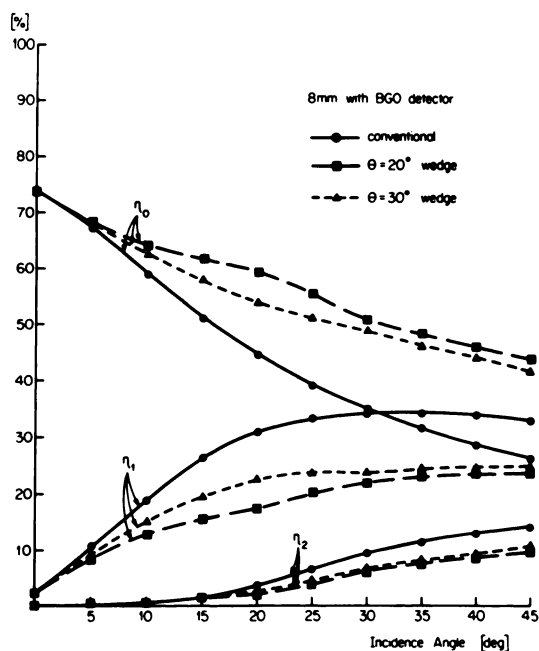


FIG. 5. Results of Monte Carlo simulation for 8-mm-wide BGO detector with conventional rectangular shape and for two wedge shapes with $\theta = 20^\circ$ and 30° . Primary detection efficiency (η_0), spillage to adjacent detector (η_1), and spillage to next-to-adjacent detector (η_2) are calculated as a function of incidence angle of photon.

as shown in Figs. 1, 2, and 3. Crystal height and length (Fig. 2a) of 2 cm and 4 cm were used, and the energy threshold was set at 350 keV to approximate practical PET operation. Two detector widths (8 and 4 mm) and three kinds of crystal shapes (20° and 30° wedges, and the parallelepiped) were tested as a function of incidence angle from 0° to 45° . In a real situation there are no incident photons from outside the wedge angle, since this angle is the largest incidence angle determined by the sizes of object and detector ring. A total of 50,000 photons were used for each simulated run.

DISCUSSION

Figures 5 and 6 are the results of the computer simulations. η_0 , η_1 , and η_2 denote respectively the detection efficiency of the primary detector (the one a given photon enters first), percent of spillage to an adjacent detector, and percent of further spillage to next-to-adjacent detector. For a detector 8 mm wide, the improvements of detection efficiency and interdetector spillage are shown in Fig. 5. For example, compared with the rectangular detector and for an incidence angle of 20° , the wedge detectors have a gain in primary detector efficiency (η_0) of as much as 33% (from 0.45 to 0.6). Considering the coincidence detection of two annihilation photons, this amounts to 78% improvement. In addition, spillage to an adjacent detector (η_1) is also reduced from 33% to 17%. For a detector 4 mm wide (Fig. 6), the ratio of primary detector efficiency (η_0) to spillage into an ad-

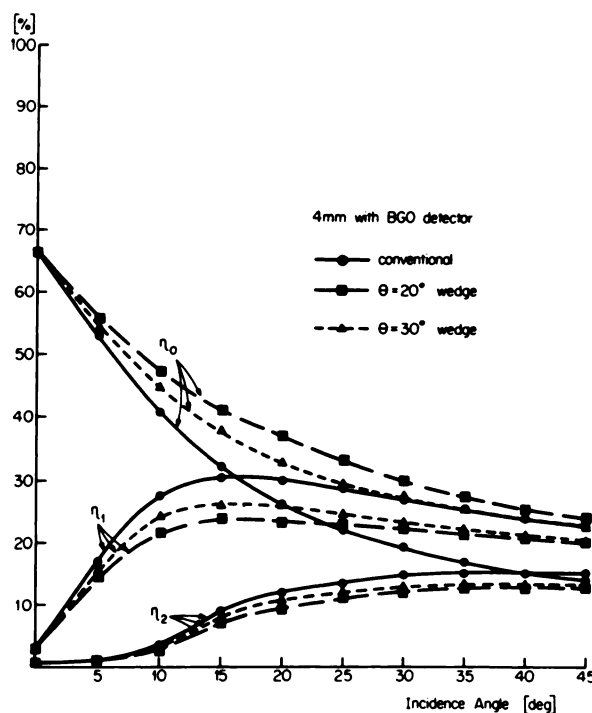


FIG. 6. Same as Fig. 5 but for detector width 4 mm.

acent detector (η_1) for a 20° wedge is also improved markedly ($0.38/0.23 = 1.61$).

CONCLUSION

By giving a wedge shape to the front end of a detecting crystal, especially one with the high stopping power of BGO, detection efficiency as well as spatial resolution can be improved, due to the increase of absorption length for photons incident at an oblique angle. By a Monte Carlo simulation, a 33% increase in primary detection efficiency and 54% decrease in spillage to an adjacent detector are observed for the case of a detector 8 mm wide. This should contribute to the uniformity of reconstructed images as well as to sensitivity. Considering the sensitivity improvement and prevention of interdetector spillage, which lead to the improvement of resolution and uniformity, especially for a narrow-width BGO scintillation detector, the wedge-shaped crystal should be an important asset in future high-resolution PET development.

REFERENCE

1. CHO ZH, CHAN J, ERIKSSON L: Circular ring transaxial positron camera for 3-D reconstruction of radionuclide distribution. *IEEE Trans Nucl Sci* NS-23:1 613-622, 1976
2. CHO ZH, HILAL SK, CORRELL JW: High resolution spherical positron tomography with bismuth germanate scintillation crystals. *Med Phys* 7:433, 1980
3. TER-POGOSSIAN MM: Special characteristics and potential for dynamic function studies with PET. *Semin Nucl Med* 1:13-23, 1981
4. ERIKSSON L, BOHM C, KESSELBERG M, et al: A four-ring

- positron camera system for emission tomography of the brain. *IEEE Trans Nucl Sci* NS-29: No 1, 539-543, 1982
5. BUDINGER TF, DERENZO SE, HUESMAN RH, et al: Positron emission tomography: Instrumentation perspectives. In *Proceedings of International Workshop on Physics and Engineering in medical imaging*, Nalcioglu O, Pueruitt J, eds. New York, IEEE Computer Society Press, 1982, pp 3-13
 6. CHO ZH, FARUKHI MR: Bismuth Germanate as a potential scintillation detector in positron camera. *J Nucl Med* 18: 840-844, 1977
 7. MOSZYNSKI M, GRESSET C, VACHER J, et al: Timing properties of BGO scintillator. *Nucl Instrum Meth* 188: 403-409, 1981
 8. NAHMIAS C, KENYON DB, GARNETT ES: Optimization of crystal size in emission computed tomography. *IEEE Trans Nucl Sci* NS-27:529-532, 1980
 9. DERENZO SE: Monte Carlo calculations of the detection efficiency of arrays of NaI(Tl), BGO, CsF, Ge, and plastic detectors for 511 keV photons. *IEEE Trans Nucl Sci* NS-28:131-136, 1980
 10. NAHMIAS C, KENYON DB, GARNETT ES: Experience with a high efficiency positron emission tomograph. *IEEE Trans Nucl Sci* NS-29:548-550, 1982
 11. BROOKS RA, SANK VJ, FRIAUF WS, et al: Design considerations for positron emission tomography. *IEEE Trans Biomed Eng* BME-28: No. 2, 158-177, 1981

Erratum

In the article entitled, "The Walsh-Hadamard Transform: An Alternative Means of Obtaining Phase and Amplitude Maps," Vol. 25, May 1984, pp. 608-612, two errors occurred which are corrected below.

On page 610, in the first paragraph, the second sentence should read as follows:

The algorithm used in the computer* is the trigonometric form of DFT, where Eqs. (1) and (2) have been applied with $K = 1$ and $N = 16, 24$.

On page 611, reference is made to Table 1, which was inadvertently omitted. Shown below is the complete table.

TABLE 1. RESULTS OF COMPARISON BETWEEN DFT AND WHT FOR DIFFERENT PARAMETERS IN 30 STUDIES

Parameters	DFT	WHT	r*	Differences
†Computing time (seconds)	109.5 ± 8.3	64.6 ± 4.7	0.994	43.4 ± 3.6
†Left ventricle mean value of phase (degrees)	115 ± 20	105 ± 20	0.995	10
Standard deviation of phases in left ventricle (degrees)	22	22	0.99	—
†Maximum value of amplitude in left ventricle (counts per pixel)	382 ± 198	490 ± 252	0.998	- 108 (28%)

*Correlation coefficient.
†Mean ± standard deviation.

Erratum

The following subchairman and reviewers of the peripheral vascular papers for the 31st Annual Meeting in Los Angeles were inadvertently omitted from the May issue of the *Journal of Nuclear Medicine* and from the final program:

Michael E. Siegel, M.D., Subchairman
Charles A. Stewart, M.D.
Ung Yun Ryo, M.D., Ph.D.
Robert E. Henry, M.D.

Erratum

In the May 1984 issue of the *Journal of Nuclear Medicine*, reference to an abstract appearing in that issue was inadvertently omitted in the Author Index under Thakur, ML. Dr. Thakur was co-author of "Platelet Labeling in Plasma Made Simple and Efficient: Preparation and Evaluation," appearing on P65.